CPUE standardization of yellowfin tuna caught by Korean tuna longline fishery in the Indian Ocean, 1979-2019

Sung Il Lee, Junghyun Lim, Mi Kyung Lee and Youjung Kwon

[1]National Institute of Fisheries Science, Busan, Republic of Korea

Abstract

In this study we standardized CPUE of yellowfin tuna caught by Korean tuna longline fishery in the Indian Ocean using a lognormal constant model with added cluster factor as a categorical variable for addressing target changes over time.

Introduction

In the Indian Ocean, yellowfin tuna has been one of the highest catch in Korean tuna longline fishery along with bigeye tuna. Yellowfin catch had increased considerably since the mid-1960s and peaked at about 31 thousand tons in 1977, but it decreased with fluctuations to a few hundred tons in the early 2010s (Lee et al. 2019). Since 2014 it has increased to around 1.6 thousand tons in average for 2018-2020. This document provides results of CPUE (catch per unit effort) standardization of yellowfin tuna caught by Korean tuna longline fishery in the Indian Ocean as well as clustering analysis for addressing target changes over time using methods developed by a trilateral collaborative study (Kitakado et al. 2021).

Data and Method

Catch and effort data used in this study were collected from logbooks filled out by captains onboard. The data were plotted to explore changes in geographical distributions of efforts and yellowfin catch of Korean tuna longline fishery in the Indian Ocean.

To address target changes over time, a clustering approach was used as in the previous study (Hoyle et al. 2019) and the method is described in detail in Kitakado et al. (2021). Data used for clustering analysis contain vessel id, operation date, operation location to 1°, number of hooks and floats, and catch by species in number for albacore (ALB), bigeye (BET), yellowfin (YFT), Atlantic bluefin tuna (BFT), southern bluefin tuna (SBT), black marlin

(BLM), blue marlin (BUM), swordfish (SWO), other billfishes (BIL), sharks (SKX) and others (OTH). Data are available from 1979 to 2019 because data prior to 1979 have no information of vessel id.

We standardized CPUE of yellowfin tuna using a lognormal constant model, and the details are described in Kitakado et al. (2021). The lognormal constant model is as follows.

$$ln(CPUE + c) \sim Year + Quarter + LatLon + Cluster + Vessel + Error$$

The definition of region for yellowfin CPUE is based on the current regional structure used for YFT stock assessment (R1b-R4; regY R2-R5) (Urtizberea, 2019). However, CPUE standardization for R3 (regY R4) could not be carried out because there were not enough data to run it.

Results and Discussion

Figs. 1 and 2 show geographical distributions of fishing efforts (number of hooks) and yellowfin catch (in number) of Korean tuna longline fishery by decade from 1970s to 2010s in the Indian Ocean. The fishing efforts were concentrated in tropical areas between 10^{o}N-15^{o}S of the western Indian Ocean during the 1970s to 1990s, which targeted BET and YFT. Until the 1980s there were a little fishing efforts in the south of 25^{o}S, but since the 1990s some fishing vessels moved southward to fish for SBT in the western and eastern Indian Oceans around 35^{o}S-45^{o}S. In the 2010s, most of the fishing vessels were operated in the south of the equator and they operated mainly in the south of 20^{o}S in the western and eastern Indian Oceans to fish for YFT, BET, SBT and sometimes ALB.

Regarding Korean tuna longline fishery, three to five clusters were chosen in each region to address target strategies (4 clusters for R1b (regY R2); 5 clusters for R2 (regY R3); 5 clusters for R3 (regY R4); 3 clusters for R4 (regY R5)).

In region R1b (regY R2), most clusters were dominant before 2010. Clusters 1 and 2 were more prominent from February to May. Hooks were similar in all clusters, with clusters 2 and 4 higher (Fig. 3(A)). The species composition of cluster 1 showed higher OTH along with BET and YFT. Cluster 2 was dominated by YFT, followed by BET. Cluster 3 showed more YFT along with BET, and cluster 4 was dominated by BET, followed by YFT (Figs. 4(A) and 5(A)).

In region R2 (regY R3), clusters 3 and 4 were dominated in the early and late of the period, respectively, and cluster 5 occurred since the 1990s. Clusters 2 and 4 were more prominent in the first half of the year, and clusters 3 and 5 were prominent in the second half of the year. Hooks were similar in all clusters. Cluster 3 was formed in the northeast area, and clusters 5 in the southwest area, compared to other clusters (Fig. 3(B)). The species composition of cluster 1 had more YFT along with ALB and BET, cluster 2 was dominated by YFT, and cluster 3 was dominated by BET along with some YFT. Cluster 4 had similar amounts of YFT and OTH, and cluster 5 was dominated by SBT (Figs. 4(B) and 5(B))

In region R3 (regY R4), clusters 1 and 3 occurred since the 1990s, clusters 2, 3 and 4 were apparent in the late of the time series, and cluster 5 was apparent in the early of the time series. All Clusters except cluster 2 were more prominent in the second half of the year. Hooks were similar in all clusters, with clusters 1, 3 and 4 higher (Fig. 3(C)). Cluster 3 was formed in the north area, compared to other clusters. The species composition of cluster 1 was comprised of mostly SBT along with some ALB, cluster 2 was dominated by ALB, and cluster 3 showed higher SKX along with SBT and BET. Cluster 4 had SBT along with similar amount of OTH, and cluster 5 was dominated by BET, followed by ALB (Figs. 4(C) and 5(C)).

In region R4 (regY R5), all clusters were apparent in the early of the period and in the second half of the year. Hooks were similar in all clusters (Fig. 3(D)). The species composition of cluster 1 was dominated by BET, followed by YFT, cluster 2 was comprised of mainly BET along with some YFT, and cluster 3 had YFT along with similar amount of BET (Figs. 4(D) and 5(D)).

Fig. 6 represents YFT CPUE indices standardized by the lognormal constant model, along with the nominal CPUEs for each region. The indices showed an increase in recent years in R1b (regY R2), a stable trend in R2 (regY R3), and a decline except the middle of 2000s in R4 (regY R5). Diagnostic frequency distributions of standardized residuals and Q-Q plot indicate that data fitted the GLM well (Fig. 7).

The influence plots for each factor by the lognormal constant model for R1b (regY R2) are shown in Fig. 8. The pattern of the parameter estimates is shown at the top of each plot, and the influence of each parameter on the year effect on the right side of each plot.

References

Hoyle S, Chang ST, Fu D, Kim DN, Lee SI, Matsumoto T, Chassot E and Yeh YM. 2019.

Collaborative study of bigeye and yellowfin tuna CPUE from multiple Indian Ocean longline fleets in 2019, with consideration of discarding. IOTC-2019-WPM10-16.

Kitakado T, Wang S-P, Satoh K, Lee SI, Tsai W-P, Matsumoto T, Yokoi H, Okamoto K, Lee MK, Lim J-H, Kwon Y, Su N-J, Chang S-T and Chang F-C. 2021. Report of trilateral collaborative study among Japan, Korea and Taiwan for producing joint abundance indices for yellowfin tuna in the Indian Ocean using longline fisheries data up to 2019. IOTC-2021-WPTT23(DP)-14.

Lee SI, Kim DN, Hoyle SD. 2019. CPUE standardization of bigeye and yellowfin tuna caught by Korean tuna longline fishery in the Indian Ocean. IOTC-2019-WPTT21-29_Rev1.

Urtizberea A, Fu D, Merino G, Methot R, Cardinale M, Winker H, Walter J and Murua H. 2019. Preliminary assessment of Indian Ocean yellowfin tuna 1950-2018 (Stock Synthesis, V3.30). IOTC-2019-WPTT21-50.

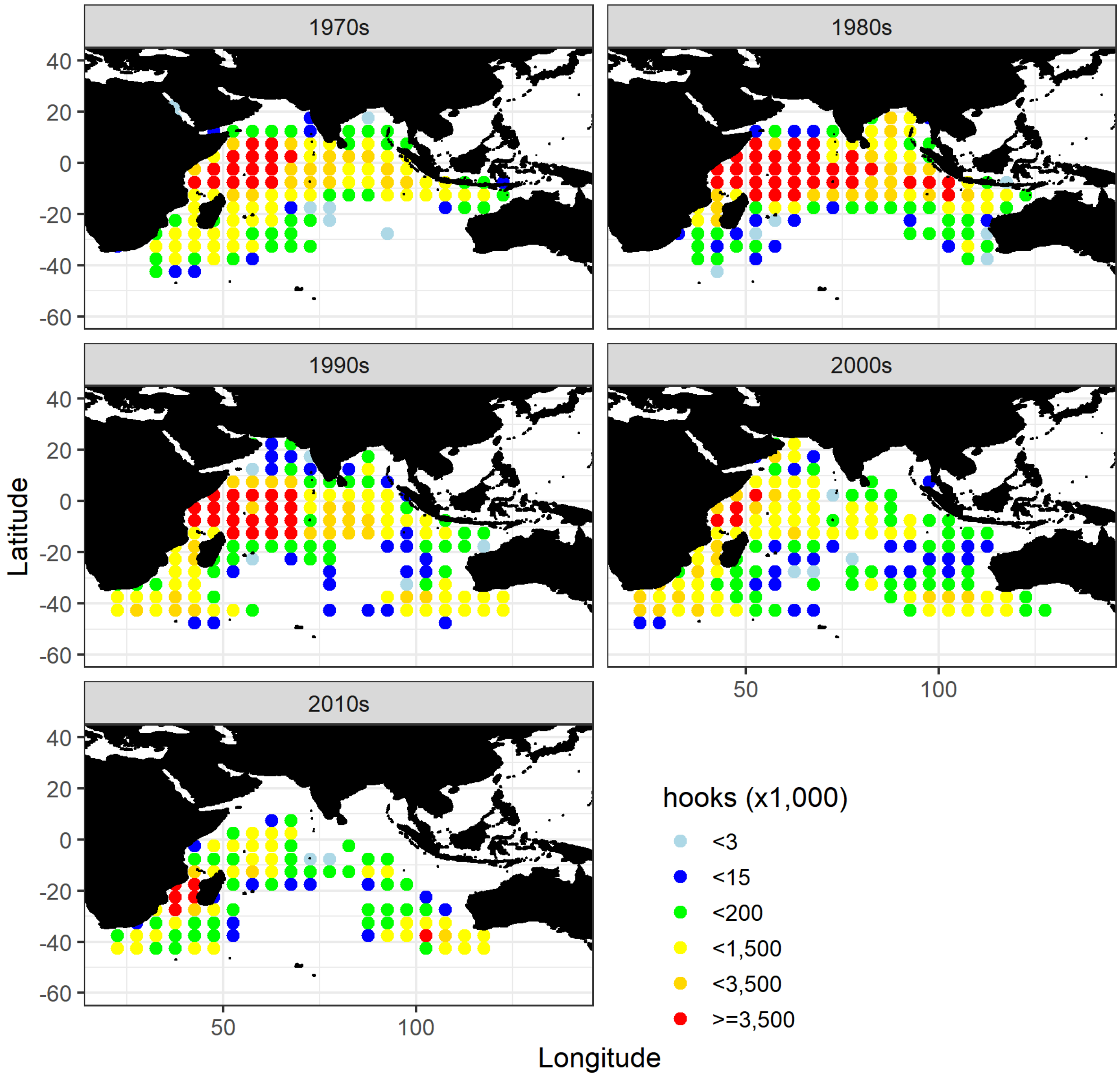

Fig. 1. The geographical distributions of total effort (number of hooks) of Korean tuna longline fishery in the Indian Ocean during the 1970s-2010s.

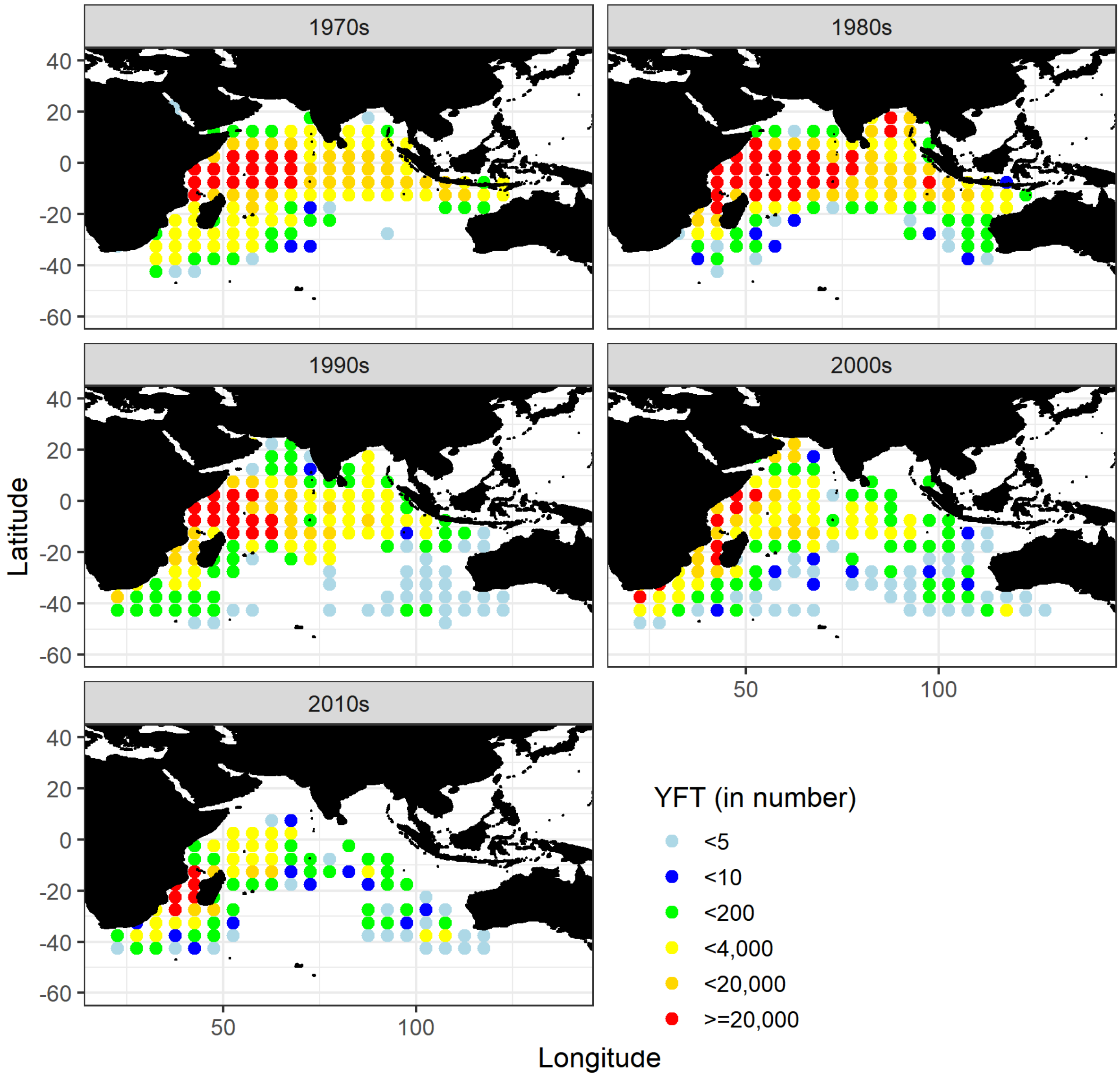

Fig. 2. The geographical distributions of yellowfin tuna caught by Korean tuna longline fishery in the Indian Ocean during the 1970s-2010s.

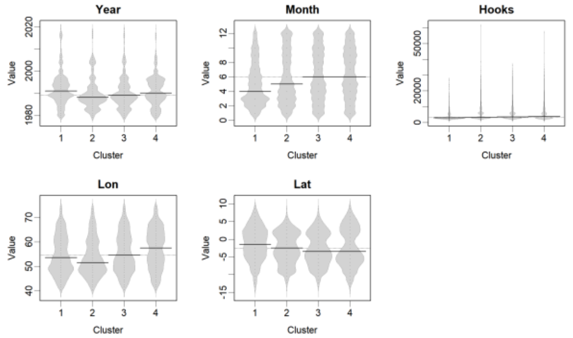

(A) R1b (regY R2)

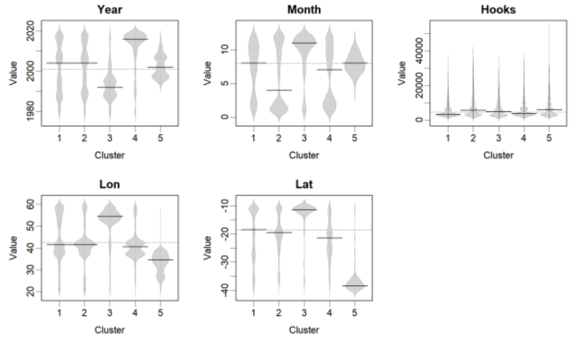

(B) R2 (regY R3)

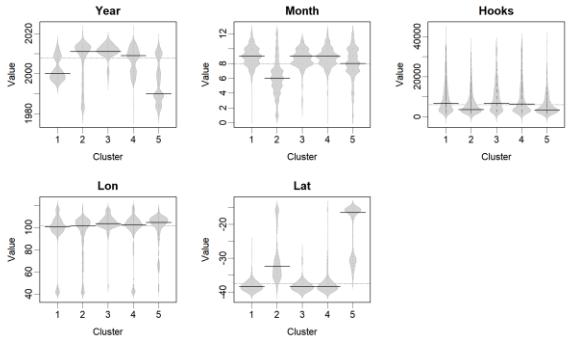

(C) R3 (regY R4)

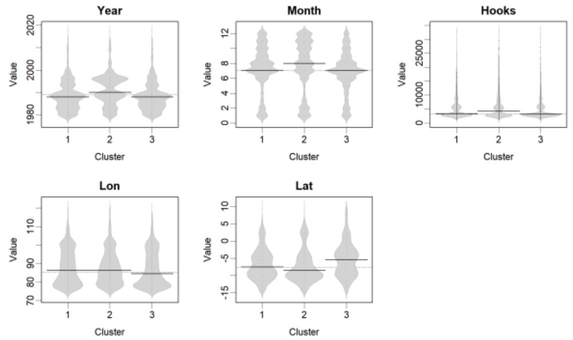

(D) R4 (regY R5)

Fig. 3. Beanplots showing the number of sets versus covariate by cluster for each region. The horizontal bar indicates the median.

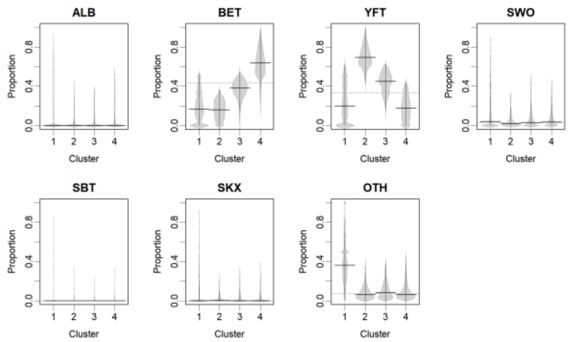

(A) R1b (regY R2)

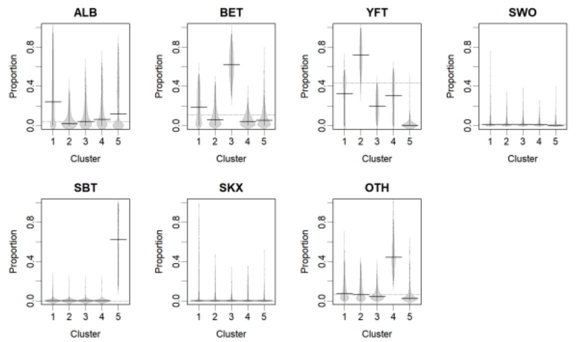

(B) R2 (regY R3)

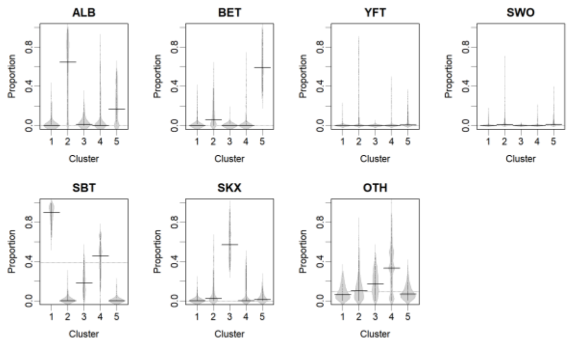

(C) R3 (regY R4)

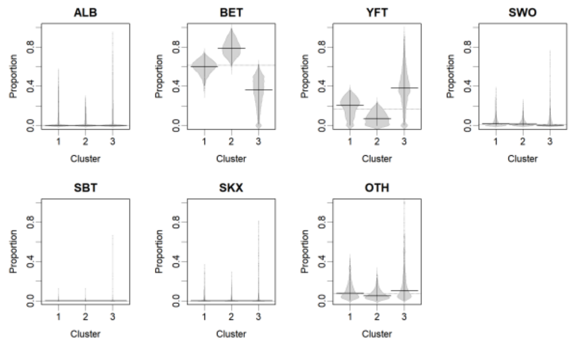

(D) R4 (regY R5)

Fig. 4. Beanplots showing species composition by cluster for each region (ALB: albacore tuna, BET: bigeye tuna, YFT: yellowfin tuna, SWO: swordfish, SBT: southern bluefin tuna, SKX: sharks, and OTH: other fishes). The horizontal bar indicates the median.

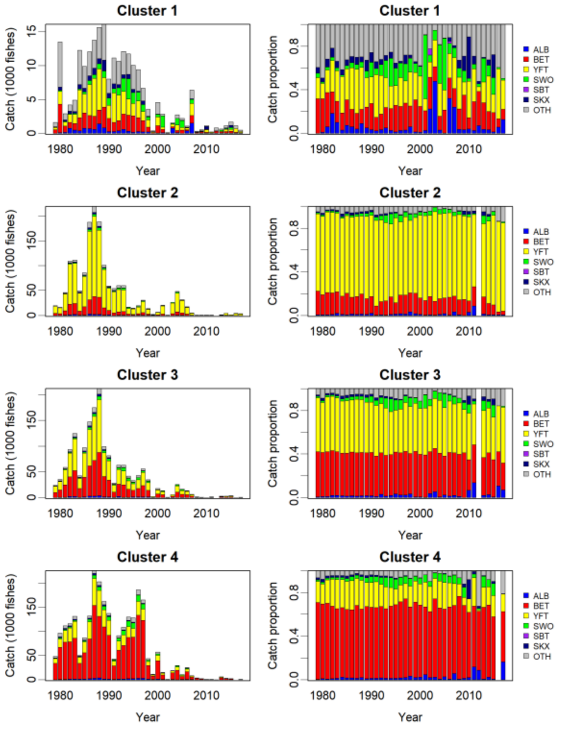

(A) R1b (regY R2)

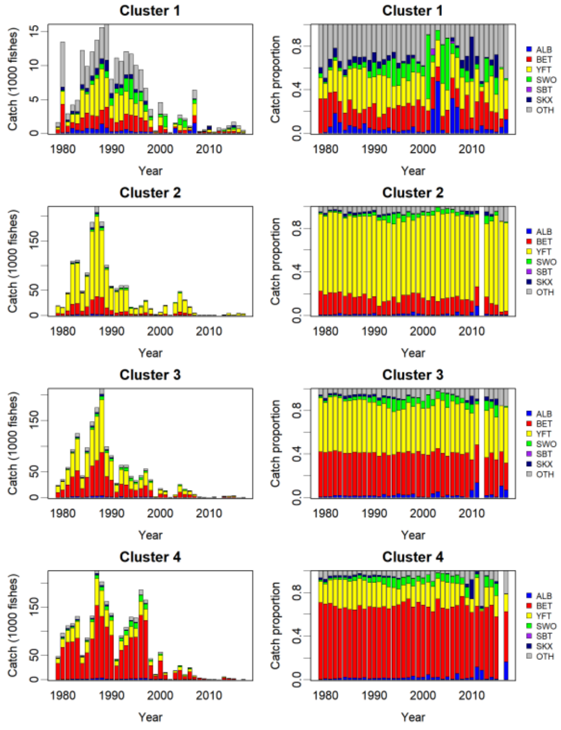

(B) R2 (regY R3)

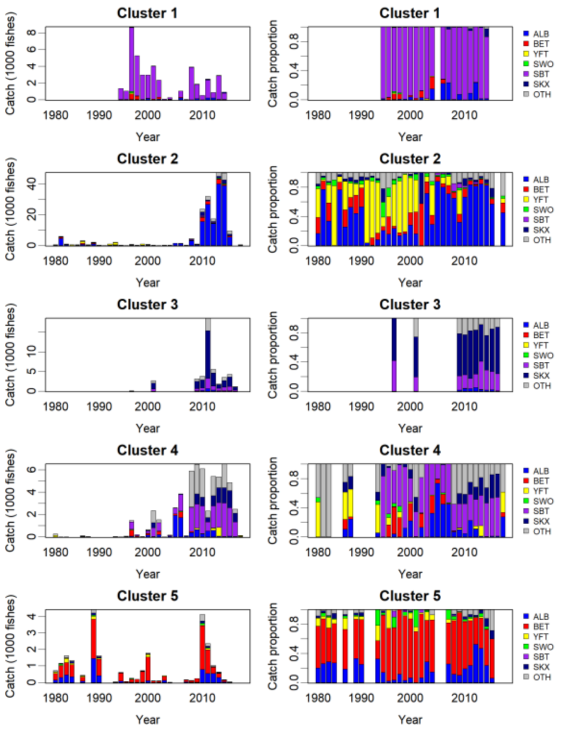

(C) R3 (regY R4)

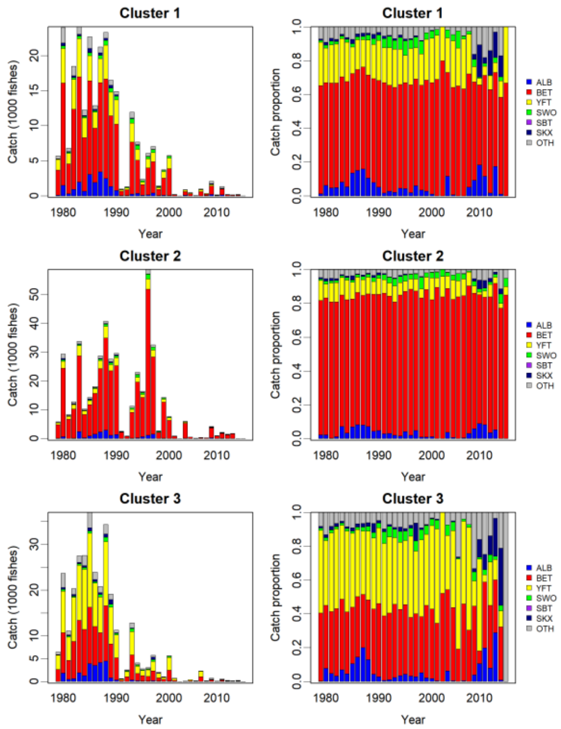

(D) R4 (regY R5)

Fig. 5. Annual change in catch and species composition by cluster for each region.

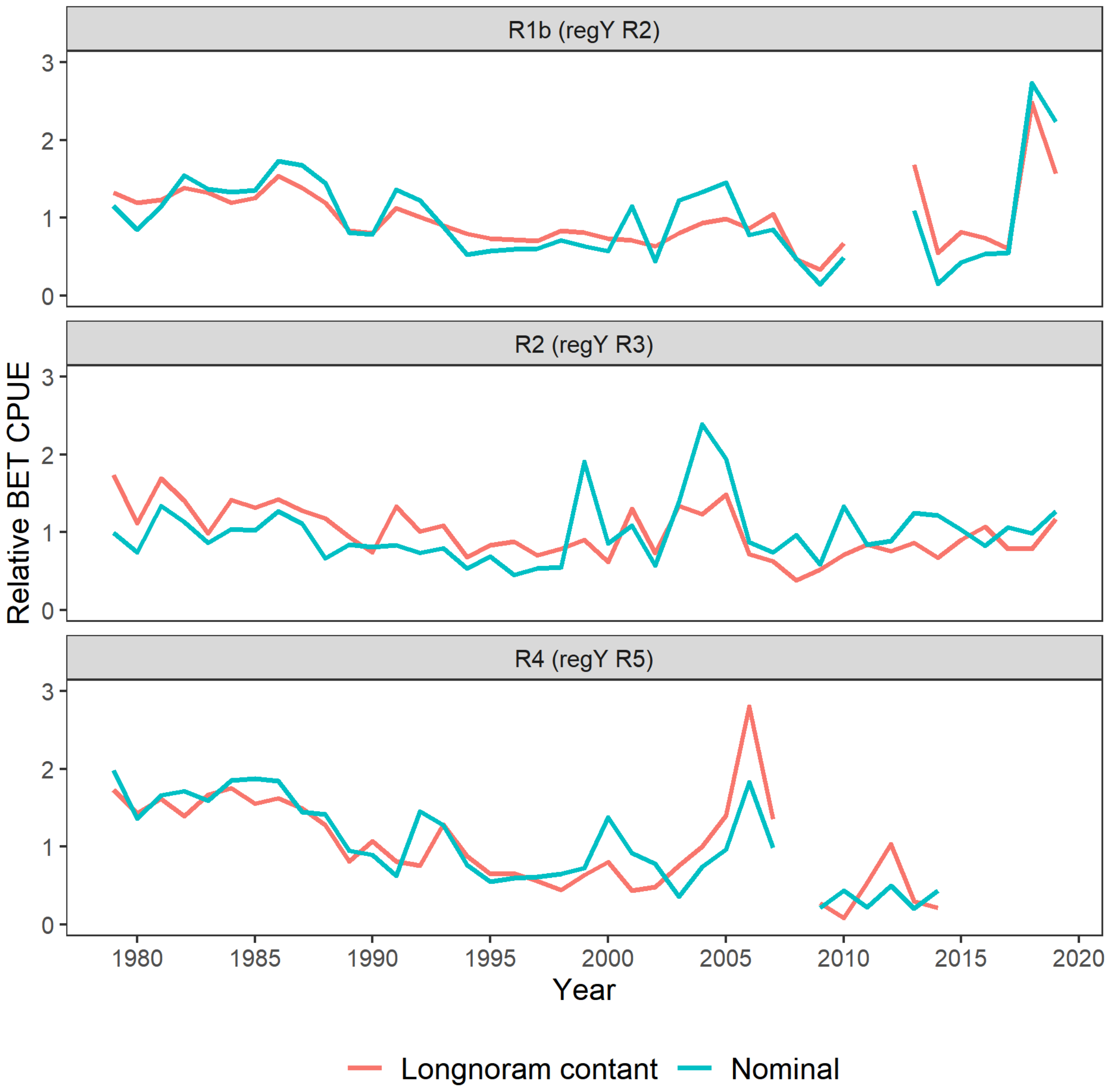

Fig. 6. Standardized yellowfin CPUE indices from Korean longline fishery by region based on the lognormal constant model.

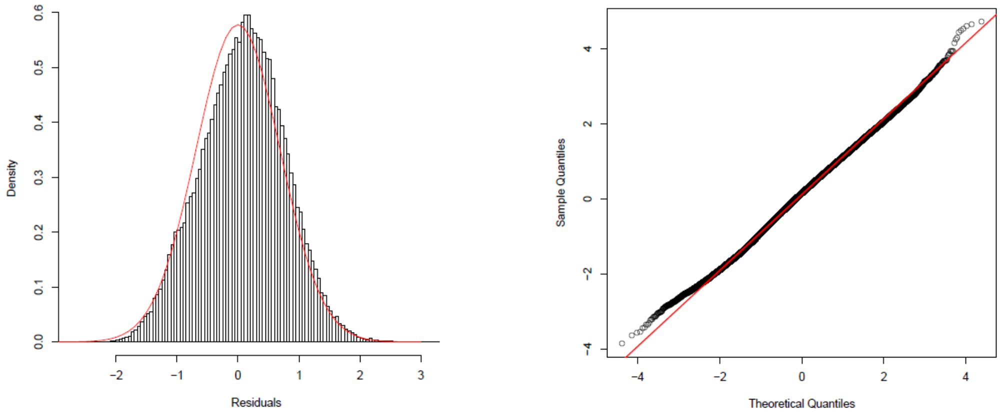

(A) R1b (regY R2)

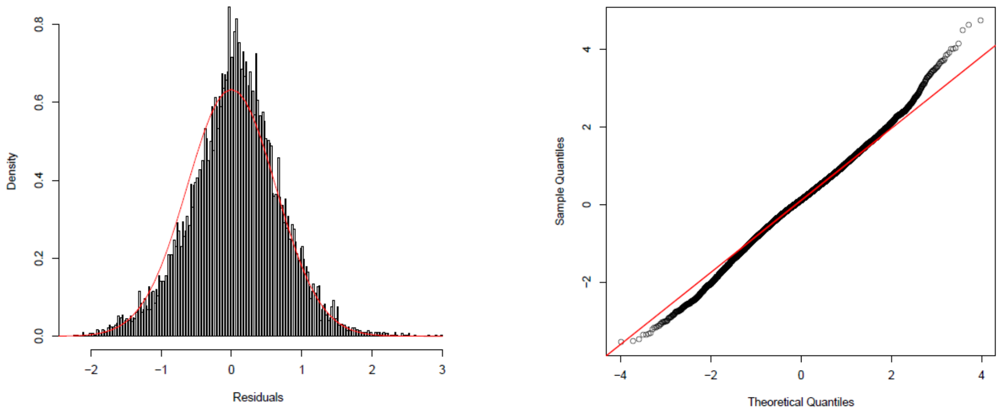

(B) R2 (regY R3)

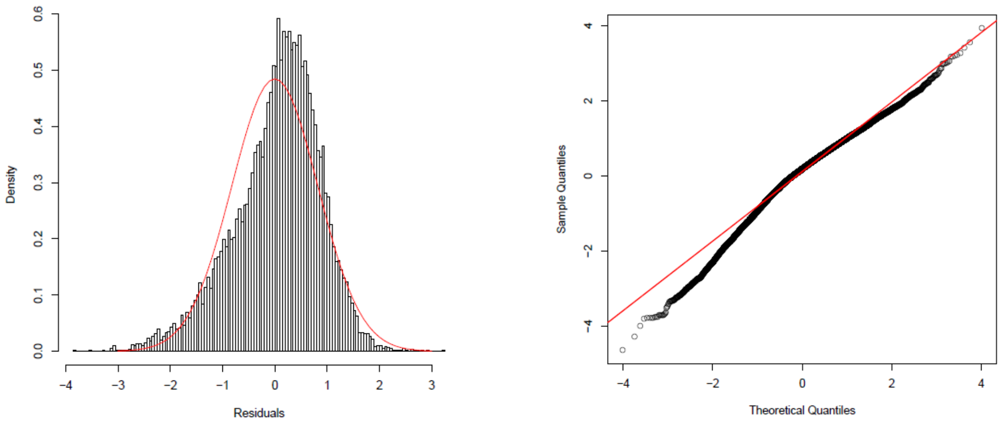

(C) R4 (regY R5)

Fig. 7. Frequency distributions of standardized residuals and Q-Q plot of yellowfin CPUE standardization for each region.

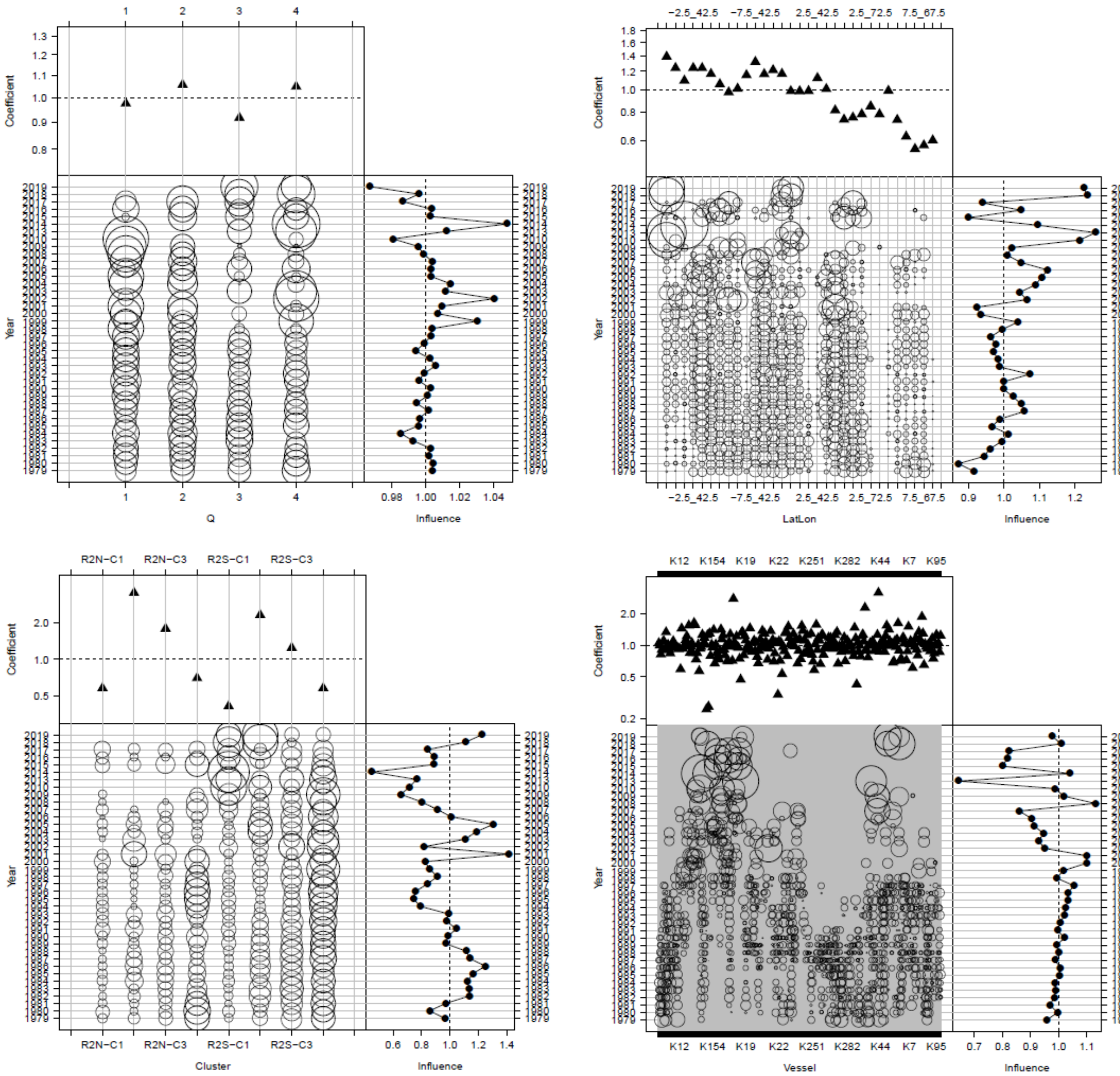

Fig. 8. Influence plots by each effect for region R1b (regY R2).